Melting Kinetics of Thermally Responsive Microgel Crystals

Shijun Tang,[†] Zhibing Hu,*[,†] Bo Zhou,[†] Zhengdong Cheng,[‡] Jianzhong Wu,[§] and Manuel Marquez[||,#]

Department of Physics, University of North Texas, Denton, Texas 76203, Artie McFerrin Department of Chemical Engineering, Texas A&M University, College Station, Texas 77843, Department of Chemical and Environmental Engineering, University of California, Riverside, California 92521, Harrington Department of Bioengineering, Arizona State University, NIST Center for Theoretical and Computational Nanosciences, Gaithersburg, Maryland 20899

Received July 26, 2007; Revised Manuscript Received September 19, 2007

ABSTRACT: The melting kinetics of three-dimensional colloidal crystals consisting of poly(*N*-isopropylacrylamide) microgels was investigated by using UV−visible transmission spectroscopy. It was found that the melting was initiated with a decrease of the interplanar spacing of the crystals and that crystallites broke into smaller pieces at large overheating temperatures. The crystallites reach a minimum burst size before completely broken apart. The complete melting occurs as the average thermal fluctuation of the particles reach around 19%. The experimental results corroborate with recent computer simulations that conciliate the Lindemann criterion of melting with Born's mechanical instability.

Introduction

Phase transition in colloidal dispersions has been of considerable interest in recent years for both theoretical and practical considerations.[1,2] Colloidal dispersions display features analogous to those occurred in atomic systems where rigorous theoretical insight into the phase behavior is limited by the many-body effects. Meanwhile, self-assembly of colloidal spheres provides a viable approach for fabrication of nanostructured materials such as membranes, catalysts, gas separation, storage media, and photonic crystals.[3,4] Whereas current understanding of the equilibrium properties of colloids is well advanced and the knowledge on nonequilibrium phase transitions is also rapidly emerging, the dynamic behavior of various phase transitions is still relatively little known.

Melting in atomic systems is one of the classical problems in phase transitions and has been studied over the past decades.[5,6] However, there are continuing efforts to explore the detailed mechanisms about this phase transition.[7,8] In contrast to atomic systems[5] and colloidal hard or charged spheres,[9−13] the poly(*N*-isopropylacrylamide) (PNIPAM) microgels studied in this work have temperature-tunable sizes and exhibit colloidal crystalline structures.[14−19] The kinetics of crystallization of PNIPAM microgels was investigated at different volume fractions by varying temperature.[20] At room temperature, the density and refractive index of these particles are close to those of surrounding water.[20] Recently, premelting at grain boundaries and dislocations within bulk PNIPAM microgel crystals has been observed by using real-time video microscopy.[7] The equilibrium phase behavior and the dynamics of PNIPAM microgel assemblies with attractive pair potentials have been studied by digital video microscopy.[21]

* Corresponding author.s:zbhu@unt.edu.
[†] Department of Physics, University of North Texas.
[‡] Artie McFerrin Department of Chemical Engineering, Texas A&M University.
[§] Department of Chemical and Environmental Engineering, University of California, Riverside.
[||] Harrington Department of Bioengineering, Arizona State University.
[#] NIST Center for Theoretical and Computational Nanosciences.

In this paper, we report measurements of the melting kinetics of three-dimensional colloidal crystals consisting of PNIPAM microgel spheres using the same UV−visible spectroscopy method developed in ref 20. By inspecting an attenuation peak that arose from the Bragg scattering of colloidal crystals, we analyzed the variations of the degree of crystallinity, the relative variation of average linear crystal dimension, the number density and volume fraction of the crystals during the course of the melting process at a number of overheated temperatures.

Experimental Section

Materials. *N*-Isopropylacrylamide was purchased from Polysciences, Inc. Dodecyl sulfate, sodium salt 98%; potassium persulfate; acrylic acid 99%; and *N*,*N*′-methylenebis(acrylamide) 99% were purchased from Aldrich. Tetramethylethylenediamine (TEMED) and potassium persulfate were bought from Bio-Rad Laboratories. Water for sample preparation was distilled and deionized to a resistance of 18.2 MΩ by a Millipore system, and filtered through a 0.22 μm filter to remove particulate matter.

Preparation of Microgels. PNIPAM microgels were prepared using a precipitation polymerization method.[22] Specifically, 3.78 g of *N*-isopropylacrylamide monomer, 0.11 g of acrylic acid (AA) monomer, 0.0665 g of methylenebis(acrylamide) (BIS) as cross-linker, and 0.106 g of sodium dodecylsulfate (SDS) as a surfactant were mixed with 240 mL of distilled and deionized water in the flask. The solution was stirred at 300 rpm for 30 min under nitrogen atmosphere. 0.166 g of potassium persulfate (KPS) dissolved in 10 mL of deionized water was added to start the polymerization reaction. The reaction was carried out at 70 °C for 4 h. After the solution had cooled to room temperature, the final reaction dispersion was exhaustively dialyzed in a dialysis tube for 7 days.

Light Scattering Measurements. The average size and size distribution of microgel particles were characterized by using dynamic light scattering measurements. The light scattering spectrometer (ALV, Co., Germany) was equipped with a helium−neon laser (Uniphase 1145P, output power of 22 mW and wavelength of 632.8 nm) as the light source. The particles undergo a continuous volume phase transition at about 34 °C, similar to a neutral or weakly ionized aqueous solution of PNIPAM polymers.[23]

UV—Visible Spectroscopy Measurements. The colloidal crystal was prepared by evaporating the solvent in PNIPAM dispersion

10.1021/ma0716682 CCC: $37.00
Published on Web 11/22/2007

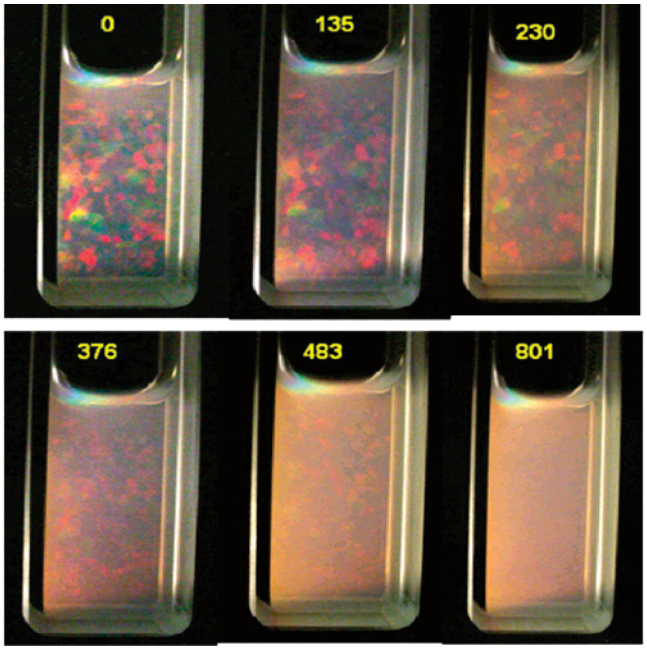

Figure 1. Progressive appearance during the melting of crystallites consisting of PNIPAM microgel spheres after the sample was heated from 19 to 27 °C. From left to right, the duration of melting is in seconds.

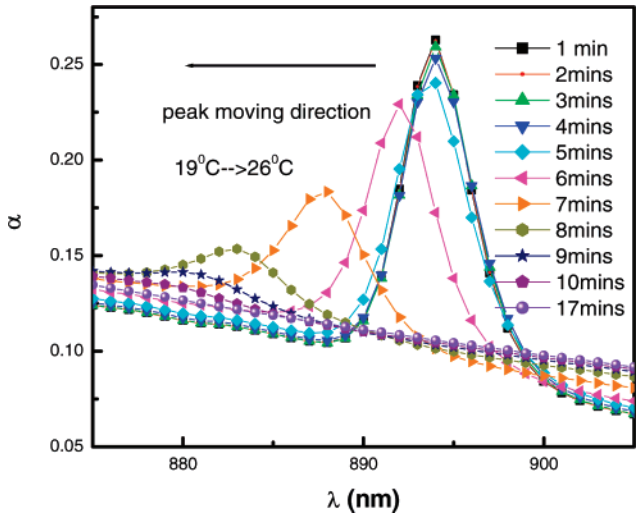

Figure 2. UV−visible spectra of the PNIPAM microgel dispersion after the sample was heated from 19 to 26 °C.

at a temperature higher than 34 °C and then allowing the concentrated dispersion to reach an equilibrium state at 19 °C for 1 week. The dispersion of the PNIPAM particles at pH about 4.4 was put into a quartz cuvette with interior dimensions of 45 × 10 × 10 mm and wall thickness of 1 mm. The crystalline grains or crystallites gradually appeared and grew in size at this temperature. Previous neutron scattering experiment revealed that the PNIPAM colloidal crystal exhibits a face centered cubic (fcc) structure.[16] Before each measurement, the sample was kept at 19 °C for about 24 h and then submerged into a heat bath at four different temperatures 28, 27, 26, and 25 °C. The kinetics of melting of the PNIPAM colloidal crystal was monitored by measuring UV−visible transmission spectra on a diode array spectrometer (Hewlett-Parkard, model 8543) with the wavelengths ranging from 190 to 1100 nm. The turbidity of the samples was obtained from the ratio of the transmitted light intensity (I_t) to the incident intensity (I_0) as $\tau = -(1/a)\ln(I_t/I_0)$, where a is the sample thickness (1 cm). In the crystal phase, the UV−visible spectrum exhibits a sharp attenuation peak due to Bragg diffraction. The structure factors $S_B(\lambda,t)$ were

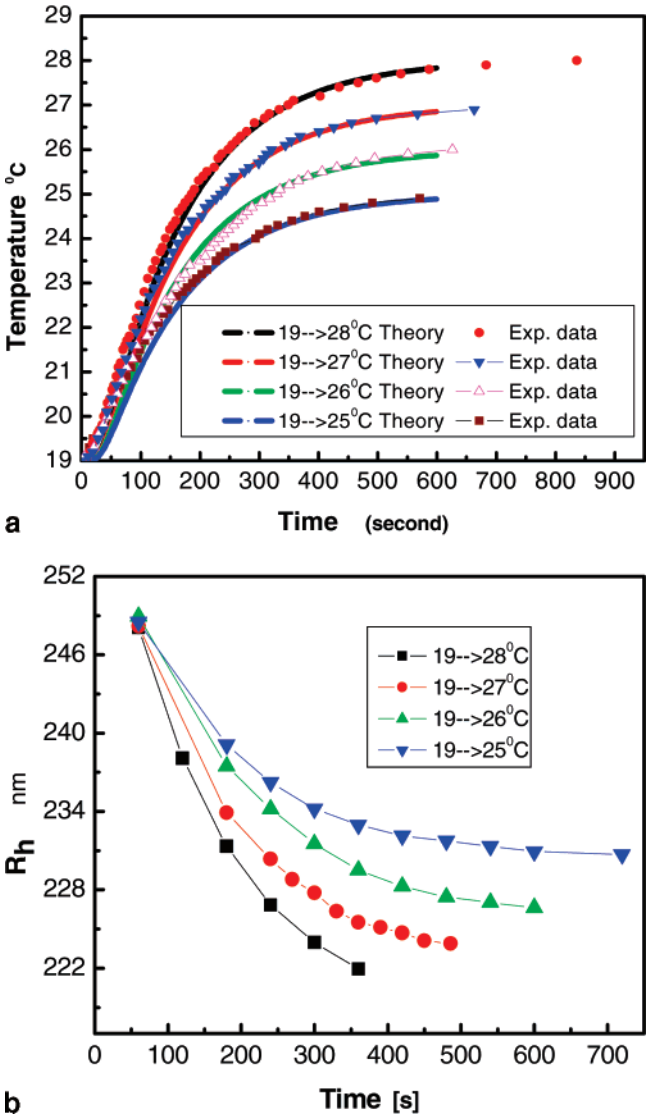

Figure 3. (a) Temperature at the center of the sample cell as a function of time after the sample cell was heated from the initial to the final temperature. Solid lines are obtained by the numerical calculation using the thermal diffusion equation and parameters listed in the paper. (b) Hydrodynamic radius of microgels as a function of time is determined by combining Figure 3a and the relation of $R_h = 332.77 - 4.09T$ in the temperatures ranging from 12 to 29 °C.

obtained by subtracting the background from the transmission spectra following a reported method.[24,25]

Theoretical Section

The degree of crystallinity, $X(t)$, defined as the volume fraction of crystallites in the sample, is related to the area of the Bragg peak[25−26]

$$X(t) = \kappa \int_{\Delta\lambda} S_B(\lambda,t)\, d\lambda \qquad (1)$$

where κ is a normalization constant and $S_B(\lambda,t)$ are the structure factors of the colloidal crystals. The normalization constant is obtained by considering that $X(t_f{=}24h){=}1$ at 19 °C at which the particle dispersion is fully crystallized. The relative change of average linear crystallite size $L(t)$ (in units of sphere diameter $2R$) with time is obtained from the width of the Bragg peak at half-maximum,

$$L(t) = \frac{\pi K}{\Delta q(t) R} \qquad (2)$$

where $K = 1.155$ is the Scherrer constant for a crystal of cubic shape and $\Delta q(t)$ is associated with the width of the peak at half-maximum. As a dimensionless quantity, $L(t)$ describes the change of average linear crystallite size relative to the average particle size. In this paper, $L(t)$, $R(t)$, and $\phi(t)$ delineate the relative variation of average linear size of crystal, mean particle size, and average effective volume fraction at the certain time, respectively.

The number density of (relatively average sized) crystallites are calculated from

$$N(t) = X(t)/L^3(t) \tag{3}$$

The volume fraction Φ_c of microgel particles in the crystalline state is given by

$$\Phi_c(t) = 0.0130[q_m(t)R]^3 \tag{4}$$

where $q_m(t)$ is the scattering wave vector corresponding to the peak at time t. The same equations from (1) to (4) have been used for the analysis of crystallization kinetics.[20] For PNIPAM colloidal crystals, there is a strong, sharp peak in UV−visible spectra.[14,17,19] This peak is caused by Bragg light diffraction from the microgel crystalline structure and makes the following analysis possible.

Results and Discussion

Figure 1 shows representative snapshots of the colloidal crystal consisting of PNIPAM microgel spheres as the sample was suddenly heated from 19 to 27 °C. The polymer concentration in the microgels is about 1.8 wt %. The turbidity as a function of wavelength during the melting process is shown in Figure 2. The evolution of the Bragg peak reflects the crystalline progress in the suspension when melted. With increasing temperature, the wavelength (λ) corresponding to the Bragg peak position decreases (blue shift).

The diffraction from the ordered colloidal arrays is associated with a lattice spacing on the order of the wavelength of visible light according to Bragg's law:[14] $2nd \sin\theta = m\lambda$. The blue shift of the Bragg peak as shown in Figure 2 is not due to the

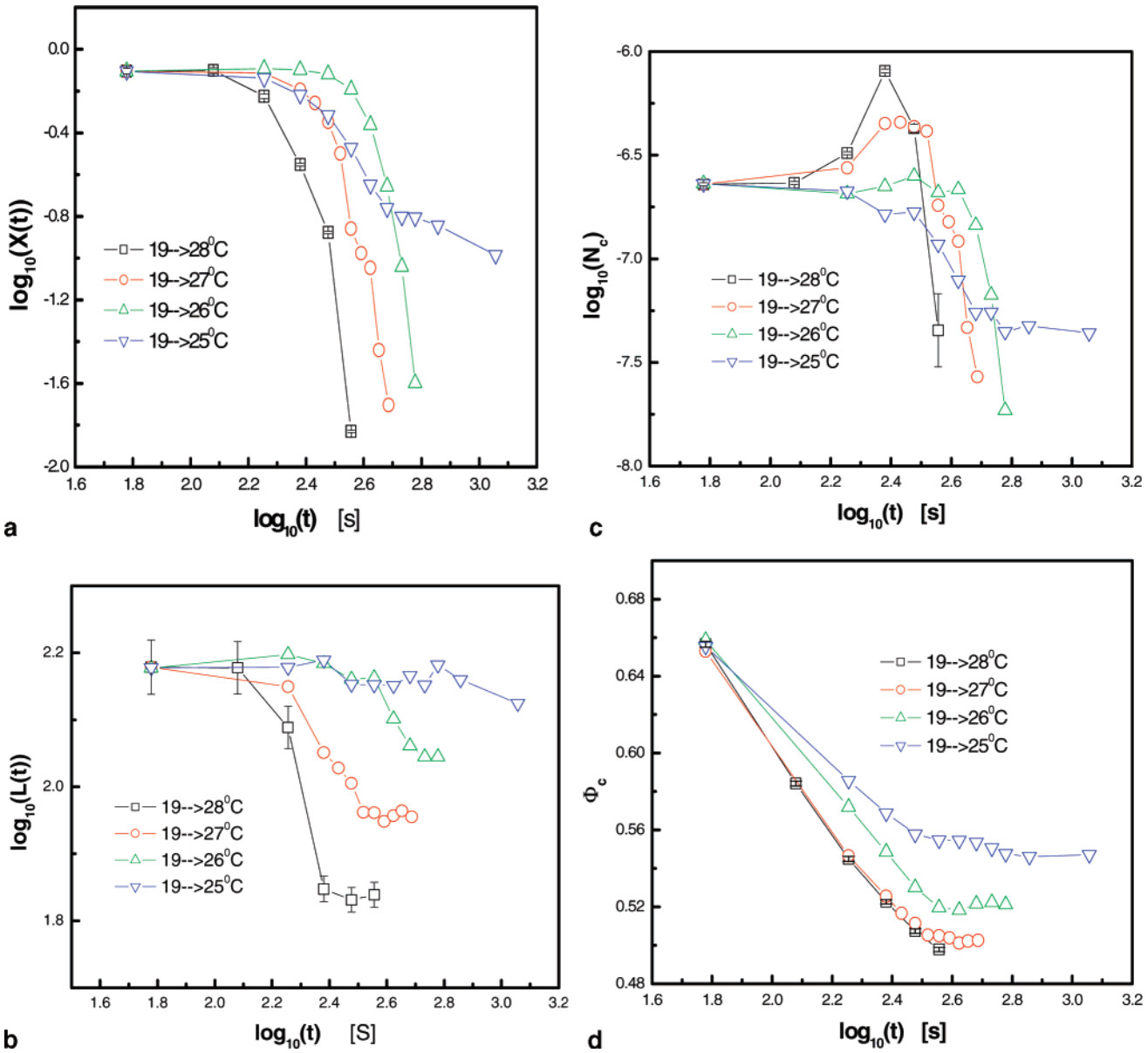

Figure 4. Dynamics of melting for colloidal crystals consisting of poly(*N*-isopropylacrylamide) microgel spheres at various overheating temperatures. Key: (a) degree of crystallinity $X(t)$, (b) the relative variation of averaged linear crystal dimension $L(t)$, (c) the variation of number density of crystallites $N(t)$, and (d) the volume fraction of the crystal phase $\Phi_c(t)$.

change of the refractive index introduced by shrinkage of microgels as the temperature is increased from 19 to 26 °C. The reduction of particle size would slightly raise the refractive index thus lead to a small red-shift of the Bragg peak. Therefore, the blue shift of the Bragg peak is attributed to the decrease of the lattice spacing induced by the shrinking particles. In order to retain the osmotic pressure of the crystalline phase in balance with the liquid phase in the suspension, the reduction of the particle size must be compensated by the decreasing of the lattice spacing. The significant lattice contraction during melting was not observed in hard-like colloidal systems before.

The hydrodynamic radius of the microgel in a dilute dispersion as a function of temperature was determined by dynamic light scattering measurements and fitted by a relation of $R_h = 332.77 - 4.09T$, where T is the temperature ranging from 12 to 29 °C. The change of particle size under a sudden temperature jump is determined by measuring the temperature variation of the sample in the cell as a function of time. Since the microgel dispersion is mostly composed of the water (about 97 wt %), its thermal diffusion coefficient is essentially the same as that of water, which is 0.14 mm^2/s at 20 °C. The physical properties of the quartz standard cell from Fisher Corporation are: heat conductivity $k = 1.38$ W/mK, density $\rho = 2201-2600$ Kg/m^3, specific heat $c = 700-770$ J/kg·K, and thermal diffusive coefficient $= 0.69-0.90$ mm^2/s. The thickness of the quartz wall was 1 mm and the distance from quartz wall to the center was 5 mm. A thermometer was placed in the center of the cell and was used to monitor the temperature change as shown in Figure 3a. The numerical solutions obtained from the heat equation match the experimental data very well (solid lines, Figure 3a). Combining the temperature vs time relation (Figure 3a) and R_h vs temperature relation ($R_h = 332.77 - 4.09T$), we have determined the relation between the particle radius and the time under a sudden temperature jump as shown in Figure 3b. For a concentrated dispersion, the particle size is generally smaller. The mean particle size $R(t)$ in the crystal phase is further approximately corrected by multiplying 0.778 following a treatment in a neutron scattering experiment.[16] This correction also worked well for crystallization kinetics.[20] From the reduced osmotic second virial coefficient from the static light scattering and from the calculation, the PNIPAM microgels can be considered as a hard sphere system below the critical solution temperature.[19] This temperature and time dependent radius was then used for data analysis.

Figure 4a shows that after a brief thermal relaxation, the degree of crystallites, $X(t)$, declines rapidly as the sample was heated from 19 to 28, 27, and 26 °C. We have chosen the constant κ such that $X(t_f) = 1$ as the particles form a complete crystalline lattice at 19 °C. For $X(t) < 1$, this means that the dispersion does not get fully crystallized. Some crystallites were lost due to transferring the sample from one thermal bath to another one at the UV−visible spectrometer. However, close to the melting temperature (at 25 °C), the declining rate of $X(t)$ is slow. As the temperature was increased from 19 °C to a higher value, a thermal transfer process as described by Figure 3a took place from the wall to the center of the sample cell. During the initial time (2−3 min) corresponding the flat stage in Figure 4 (parts a−c), $X(t)$, $L(t)$, and $N(t)$ do not change significantly. At the initial stage, the decrease of the volume fraction of crystal phase indicates that the particles in crystallites absorb thermal energy and begin to shrink.

Figure 4b depicts the relative variation of average linear crystallite size $L(t)$ as a function of time. $L(t)$ exhibits a plateau before completely melting at 19 to 28, 27, and 26 °C, suggesting that the crystallite kept a minimum value (L_{min}) before completely breaking apart. As the overheating temperature ΔT increases, the crystallite sizes decrease faster while the value of L_{min} is smaller.

The number density $N(t)$ of crystallites, calculated from eq 3, is shown in Figure 4c. A striking feature is that for large overheating temperatures (19 to 28 °C and 19 to 27 °C), $N(t)$ shows a maximum in the early state and then rapidly decreases with time. The increase of $N(t)$ suggests the crystallites break into the many smaller pieces. That is, a single crystal may collapse into two or three crystals separated by the fluid phase. The decrease of $N(t)$ indicates the complete melting of some crystallites, as expected during melting.

The volume fraction Φ_c of microgel particles in the crystal state is calculated from eq 4 and shown in Figure 4d. As ΔT increases, Φ_c decreases more rapidly. From 19 to above 25 °C, the colloidal crystallites completely melted, while from 19 to 25 °C, the crystallites did not completely melt. Specifically, at around 25 °C, Φ_c decreases slowly and remains near 0.55, the equilibrium crystal volume fraction. However, other overheated crystallites (19→26, 27, and 28 °C) reach metastable volume fraction (below 0.55) before completely melted as shown in Figure 4d. Instrumental errors for the hydrodynamic radius measured by dynamic light scattering, turbidity, and wavelength measured by a UV−vis spectrophotometer are about ±4 nm, ±0.02 cm^{-1}, and ±0.5 nm, respectively.[20] The error bars were estimated by analyzing error propagation in eqs 1−4, as shown in Figure 4a−d for measurements from 19 to 28 °C. The error bars should be similar for measurements with different temperature jumps.

One simple criterion of crystal melting, originally developed by Lindemann[5] has been subjected to a number of investigations.[5,27,28] In terms of the mean-squared displacement of each particle on a crystalline lattice $\langle u^2 \rangle$, and the distance between nearest-neighboring particles $\bar{A}$, the Lindemann criterion indicates that, at the melting point, the relative thermal fluctuation is approximately given by

$$\delta_L = \frac{\sqrt{\langle u^2 \rangle}}{\bar{A}} \tag{5}$$

The experimental results δ_L for hard spheres vary from 0.10 to 0.19.[5,11,29] Following refs 30 and 31, the height of the Bragg peak in the UV−visible spectra is proportional to the Debye−Waller factor $\exp(-2M)$, with $M = q^2u^2/3$ (where $q = 4\pi[\sin(\theta)]/\lambda$). The relative thermal fluctuation for the melting of PNIPAM microgel crystals thus can be calculated.

Figure 5 depicts the relative thermal fluctuation as a function of time during the melting process. As the temperature increases from 19 to 25 °C, δ_L approaches to about 15%, where the crystallites are in a coexistence regime and not completely melted. As the crystal heats from 19 °C to 28, 27, and 26 °C, the relative thermal fluctuation rapidly increases with time. All crystallites are completely melted when δ_L is about 19%, consistent with the microscopy experiment[7] showing that the PNIPAM microgel crystals melted as δ_L approaches 18%.

We can compare the Lindermann criterion of melting[5] with Born's mechanical instability criterion[32] experimentally. Such a comparison has been recently carried out by a computer simulation.[27] The bulk modulus of the colloidal crystal can be calculated as following:

$$B = -V\left(\frac{\partial \Pi}{\partial V}\right)_T \tag{6}$$

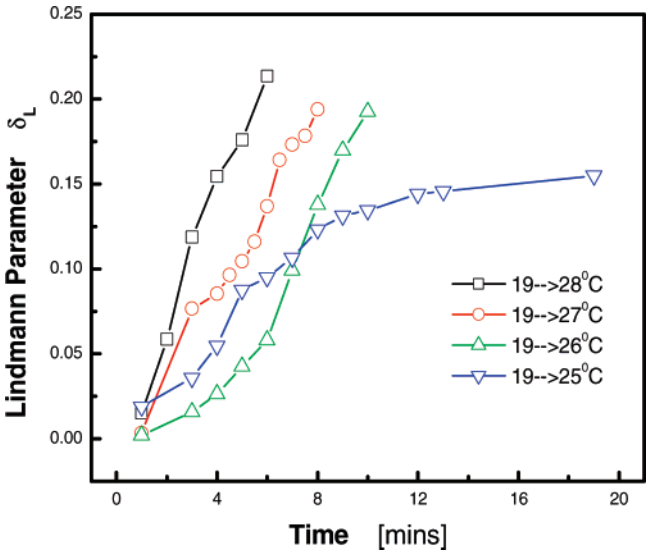

Figure 5. Lindemann parameter δ_L as a function of time of PNIPAM crystallites during the melting at different overheating temperatures.

For a face-centered cubic PNIPAM crystal, the equation of state is[33]

$$\frac{\Pi V}{NkT} = \frac{2.17}{0.738 - \Phi_c} \tag{7}$$

From eqs 4, 6, and 7, we obtain the bulk modulus of the crystalline phase:

$$B = \frac{0.005kTq_m^3}{(0.738 - \Phi_c)^2} \tag{8}$$

where q_m is the scattering wave vector corresponding to the peak. As shown in Figure 4d, the Φ_c decreases with time during melting, which results in the change of bulk modulus B. This shows that the bulk modulus decreases during the melting. Therefore, these results are consistent with the Born instability idea: melting is preceded by a continuous softening of the lattice with increasing temperature. The crystal no longer has adequate rigidity to resist melting when one of its elastic moduli is sufficiently small but not zero.[27]

Conclusions

The melting kinetics of colloidal crystal consisting of poly(*N*-isopropylacrylamide) (PNIPAM) microgel spheres has been studied by using UV−visible transmission spectroscopy. The turbidity peak in transmission spectra respect to the wavelength is related to the Bragg diffraction peak appearing at light scattering spectra. The degree of crystallite, the relative variation of average crystallite, number density of crystallites, and volume fraction of the crystal phase have been analyzed as a function of time as the crystal is overheated at different temperatures. It is found that the wavelength of the Bragg peak shifts to a shorter wavelength, indicating the decrease of interplanar spacing during the melting process. There is a striking peak of $N(t)$, indicating that crystallites are broken into smaller pieces at higher overheating temperatures. The completely melting occurs as the average thermal fluctuation δ_L reaches about 19%. The microgel crystals melt with the increase of the Lindmann parameter as well as the decrease of elastic modulus, supporting a recent computer simulation that relates the Lindemann criteria to Born's instability.

Acknowledgment. Z.H. gratefully acknowledges financial support from the National Science Foundation under Grant No. DMR-0507208. Z.D.C. acknowledges support from Texas Engineering Experiment Station and Texas A&M University.

References and Notes

(1) Russel, W. B. *Phase Transit.* **1990**, *21*, 27.
(2) Pusey, P. N. In *Liquid, Freezing, and the Glass Transition*; Les Houches, J. P., Levesque, H. D., Zinn-Justin, J., Eds.; Elsevier: Amsterdam, 1990.
(3) Xia, Y. N.; Gates, B.; Yin, Y.; Lu, Y. *Adv. Mater.* **2000**, *12*, 693.
(4) Dinsmore, A. D.; Hsu, M. F.; Nikolaides, M. G.; Marquez, Manuel; Bausch, A. R.; Weitz, D. A. *Science* **2002**, *298*, 1006.
(5) Lindemann, F. A. *Z. Phys.* **1910**, *11*, 609.
(6) Siwick, B. J.; Dwyer, J. R.; Jordan, R. E.; Miller, R. J. D. *Science* **2003**, *302*, 1382.
(7) Alsayed, A. M.; Islam, M. F.; Zhang, J.; Collings, P. J.; Yodh, A. G. *Science* **2005**, *309*, 1207.
(8) Pusey, P. N. *Science* **2005**, *309*, 1198.
(9) Hoove, W. G.; Ree, F. H. *J. Chem. Phys.* **1968**, *49*, 3609.
(10) Schaefer, W.; Ackerson, B. *Phys. Rev. Lett.* **1975**, *35*, 1448.
(11) Kuhn, P. S.; Diehl, A.; Levin, Y.; Barbosa, M. C. *Physica A* **1997**, *247*, 235.
(12) Okubo, T. *J. Chem. Phys.* **1991**, *96*, 2261. Okubo, T. *J. Chem. Phys.* **1991**, *95*, 3690.
(13) Larsen, A. E.; Grier, D. G. *Phys. Rev. Lett.* **1996**, *76*, 3862.
(14) Weissman, J. M.; Sunkara, H. B.; Tse, A. S.; Asher, S. A. *Science* **1996**, *274*, 959.
(15) Senff, H.; Richtering, W. *J. Chem. Phys.* **1999**, *111*, 1705. Senff, H.; Richtering, W. *Langmuir* **1999**, *15*, 102.
(16) Hellweg, T.; Dewhurst, C. D.; Brückner, E.; Kratz, K.; Eimer, W. *J. Colloid Polym. Sci.* **2000**, *278*, 972.
(17) Debord, S. B.; Lyon, L. *J. Phys. Chem. B* **2003**, *107*, 2927.
(18) Gao, J.; Hu, Z. B. *Langmuir* **2002**, *18*, 1360.
(19) Wu, J. Z.; Zhou, B.; Hu, Z. B. *Phys. Rev. Lett.* **2003**, *90*, 048304. Wu, J. Z.; Huang, G.; Hu, Z. B. *Macromolecules* **2003**, *36*, 440.
(20) Tang, S. J.; Hu, Z. B.; Cheng, Z. D.; Wu, J. Z. *Langmuir* **2004**, *20*, 8858.
(21) Meng, Z.; Cho, J. K.; Debord, S.; Breedveld, V.; Lyon, L. A. *J. Phys. Chem. B* **2007**, *111*, 6992.
(22) Pelton, R. H.; Chibante, P. *Colloids Surf.* **1986**, *20*, 247.
(23) Hirotsu, S.; Hirokawa, Y.; Tanaka, T. *J. Chem. Phys.* **1987**, *87*, 1392.
(24) Schätzel, K.; Ackerson, B. J. *Phys. Rev. Lett.* **1992**, *68*, 337.
(25) Harland, J. L.; Henderson, S. I.; Underwood, S. M.; van Megen, W. *Phys. Rev. Lett.* **1995**, *75*, 3572. Harland, J. L.; van Megen, W. *Phys. Rev. E* **1997**, *55*, 3054.
(26) Cheng, Z. D.; Chaikin, P. M.; Zhu, J. X.; et al. *Phys. Rev. Lett.* **2002**, *88*, 015501.
(27) Jin, Z. H.; Gumbsch, P.; Lu, K.; Ma, E. *Phys. Rev. Lett.* **2001**, *87*, 055703.
(28) Cahn, R. W. *Nature (London)* **2001**, *413*, 582.
(29) Hone, D.; Alexander, S.; Chaikin, P. M.; Pincus, P. *J. Chem. Phys.* **1983**, *79*, 1474.
(30) Debye, P. *Ann. Phys. (Leipzig)* **1914**, *43*, 49. Waller, I. *Z. Phys.* **1923**, *17*, 398.
(31) Megens, M.; Vos, W. L. *Phys. Rev. Lett.* **2001**, *86*, 4855.
(32) Born, M. *J. Chem. Phys.* **1939**, *7*, 591.
(33) Ackerson, B. J.; Schatzel, K. *Phys. Rev. E* **1995**, *52*, 6448.

MA0716682